The Eurasia Proceedings of Science, Technology, Engineering & Mathematics (EPSTEM)
ISSN: 2602-3199

The Eurasia Proceedings of Science, Technology, Engineering & Mathematics (EPSTEM), 2024

Volume 32, Pages 53-65

IConTES 2024: International Conference on Technology, Engineering and Science

Comparative Analysis of Three Converters Providing Power to a Discharge Lamp-electronic Ballast System Designed for Water Sterilization

Aicha Aissa-Bokhtache
Hassiba Benbouali University of Chlef

Maamar Latroch
Hassiba Benbouali University of Chlef

Nadia Badni
Scientific and Technical Research Center in Physico-Chemical Analysis of Tipaza

Alla Eddine Toubal-Maamar
M'hamed Bougara University of Boumerdes

Lemya Djafer
Hassiba Benbouali University of Chlef

Amina Merini
Hassiba Benbouali University of Chlef

Abstract: Water, an essential resource, has faced a continuous decline in quality over the years. Addressing this concern is crucial, and UV-C technology emerges as a fitting solution, meeting both quality treatment and environmental preservation needs. The UV bactericidal concept involves generating ultraviolet rays in a treatment chamber containing water. Ensuring a reliable power supply to low-pressure mercury-argon discharge lamps is imperative for the efficacy of UV-C disinfection. This research aims to identify the most optimal power source. To achieve this, the discharge lamp-electronic ballast system will be energized by three different converter types. The first utilizes a conventional converter with a half-bridge rectifier and inverter, employing PWM control. The second employs a 4-cell serial multicell converter, adopting a direct control strategy. The third relies on a single-phase matrix converter. Therefore, modern converters utilizing semiconductor-based switches with high switching frequencies (above 50 kHz for MOSFETs) have been used in this study.

Keywords: Electronic ballast, Half-bridge inverter, Multi-cell converter

Introduction

To obtain disinfected water, there are two main types of processes in the literature, chemical processes which use oxidants such as chlorine, generating trihalomethanes which are considered carcinogenic and physical processes which use Ultraviolet radiation. Decontamination by UV-c has a germicidal or germistatic affect without generating harmful chemical effluents for the environment, hence its undeniable advantage. It is an economical process that respects the environment. In this work, we set ourselves the goal of supplying the system of low pressure mercury-argon discharge lamp-electronic ballast in the best conditions (current source which generates a current at high frequency (50 kHz) and the most possible sinusoidal (low THD)) in order to generate the maximum UV radiation at 253.7 nm with high germicidal power.

- Selection and peer-review under responsibility of the Organizing Committee of the Conference

It seems that for discharge lamps, by increasing the supply frequency, the electrodes wear out more slowly and the life of the lamp increases. In this context, modern converters have been used consisting of switches based on semiconductor components with a high switching frequency (for MOSFETs the frequency is greater than 50 kHz). To choose the right converter for this type of application, we powered our discharge lamp-electronic ballast system with 3 different power supplies using a classic converter, a multi-cell converter and a matrix converter.

Our first system consists of an input filter (low pass), a rectifier, and a half-bridge inverter. The PWM control strategy was used. The second system is based on a serial multicell converter which implements floating capacitors whose voltages must be controlled. For this, the direct control strategy has been adopted. This new topology facilitates series connection, by ensuring a balancing of the voltages at the terminals of the switches in static mode (Aissa-Bokhtache et al., 2016; Aissa-Bokhtache et al., 2015; Aissa-Bokhtache et al., 2017). Finally we used a matrix converter, the latter allows the direct conversion of the frequency without having recourse to the continuous intermediate circuit which characterizes the conventional converters, as well as the elimination of the passive elements of storage of energy which strongly influence the intermediate circuit continuous, without forgetting that the symmetry of the matrix allows the flow of power in both directions (Costache, 2000; De Oro et al., 2014). These switching cells with fully controllable bidirectional switches provide it with frequency advantages. In order to obtain the desired amplitude and frequency, the PWM control strategy was used.

Description and Modeling of the Discharge Lamp-Electronic Ballast System

In this section, the description and modeling of the proposed discharge lamp-electronic ballast system are presented.

System Overview

Discharge lamps are devices where electrical, thermal and chemical phenomena are involved, which give rise to a complex system that is very difficult to model. The lamp power supply must be able to initiate the discharge and then control the electronic avalanche once triggered. Knowing the electrical characteristics of the load to be powered makes it possible to size the power supply for such a system. It is therefore important to establish a more detailed specification which will define the characteristics of our load.

So the supply of our system, discharge lamp-electronic ballast, must be made by a high frequency current source because the maximum UV radiation is obtained at high frequencies, (after calculation, the frequency used is 50 kHz) and with an effective arcing current of 0.65A (Aissa-Bokhtache et al., 2016). This arc current varies according to the temperature of the basin in which the lamp is immersed as well as the arc power. The maximum emission of UV radiation is achieved with a wave of 253.7 nm which is between 35 °C and 45 °C for the cold spot temperature (42 °C) (Aissa-Bokhtache et al., 2023). Figure 1 illustrates the reactor designed for water treatment using UV radiation.

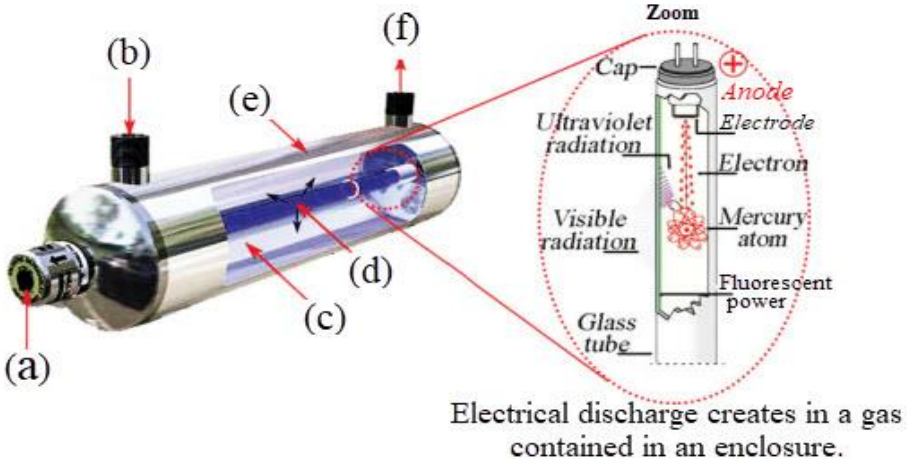

Figure 1. Reactor for water treatment by UV radiation, (a) End cap, (b) Water inlet to deal, (c) Chamber disinfection, (d) Ultraviolet rays, (e) Stainless steel chamber, (f) Disinfect water.

Model of the Electric Circuit of the Discharge Lamp

Our lamp model is represented by resistor "R_{arc}" depending of a lamp arc power and temperature and an "r_f" resistor for each cathode filament as shown in Figure 2.

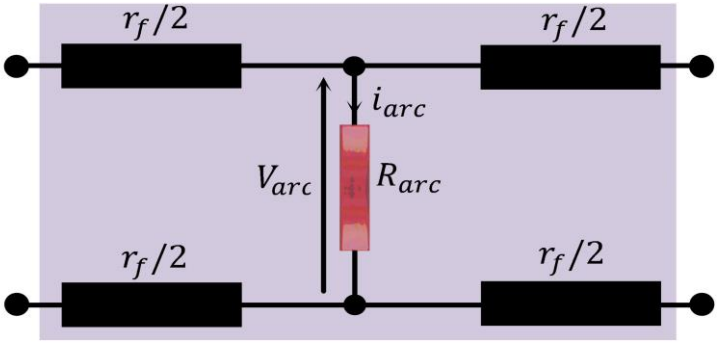

Figure 2. Model of the electric circuit of the gas-discharge lamp

Figure 3 summarizes the system studied: Discharge lamp-electronic ballast powered by a converter.

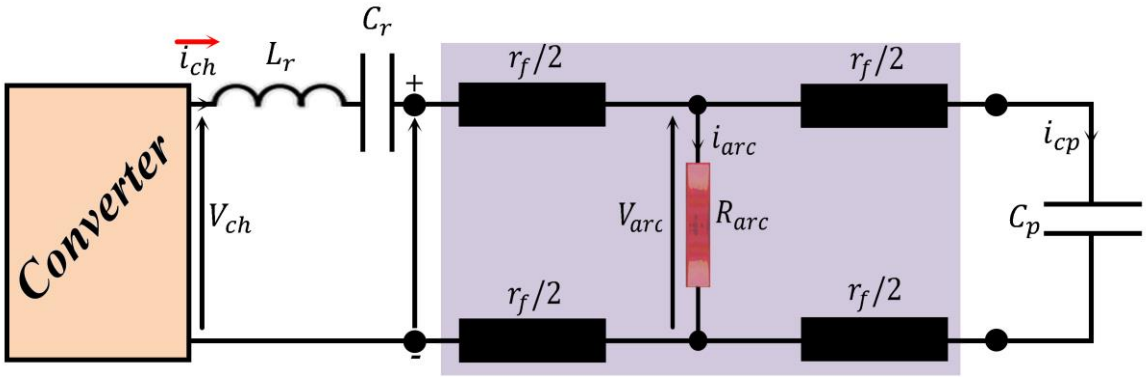

Figure 3. Equivalent circuit of electronic ballast-discharge lamp with converter

Characteristics of the Discharge Lamp

The lamp used in the simulation is a real discharge lamp described in references (Aissa Bokhtache et al., 2023), the main characteristics of the discharge lamp-electronic ballast are given in (Table1) below:

Table 1. Characteristics of the discharge lamp-electronic ballast assembly

Variables	Symbol	Values
Capacitance	C_r	*147 nF/ 250 V*
Capacitance	C_P	*8.2 nF/ 600 V*
Inductance	L_r	*1.08 mH*
Power	P_{Lamp}	*65 W*
Frequency	f	*50 KHz*
Resistance	R_{arc}	*170.769* Ω
Resistance	r_f	*5* Ω
Length	L_{tube}	*150 cm*
Current	I_{arcrms}	*0.65 A*

The consideration of R_{arc} and r_f allows us to better describe the behavior of our discharge lamp. The modeling allowed us to obtain the following transfer function, qualified as complete:

$$\frac{I_{arc}}{V_{ch}} = \frac{r_f\, C_r\, C_p\, S^2 + C_r\, S}{\left(R_{arc}+r_f\right) L_r\, C_r\, C_p\, S^3 + \left[\left(2R_{arc}+r_f\right) L_r\, C_r\, C_p + L_r\, C_r\right] S^2 + \left(R_{arc}+r_f\right)\left(C_r + C_p\right) S + 1} \quad (1)$$

With : r_f: filament resistor, R_{arc}: arc resistance, Z_{cp} : starter impedance,i_{arc}: arc current, V_{arc} :arc voltage, i_r: load current, i_{cp}: starter current, V_{lamp} :lamp voltage, L_r , C_r: resonant circuit parameters, C_p: starter capacitor. We propose to power our discharge lamp-electronic Ballast system by 3 converters to finally choose the best power supply which is in fact a current source generating a sinusoidal current with the lowest possible THD and a high frequency of 50kHz.

Method

The proposed discharge lamp-electronic ballast system is tested using three different converters, each regulating the arc current through a PI controller. Initially, the system is powered by a conventional converter. Next, it is powered by a multicell converter. Finally, the system is powered using a matrix converter.

Power Supply of the System by a Conventional Converter

Figure 4 depicts the system with a conventional converter. Characteristics of the conventional converter (Aissa Bokhtache et al., 2023) are: $C_{F1} = C_{F2} = 47\mu F/ 250$ V, $L_f = 8.2$ nF/ 600 V, and $C_f = 220$ nF / 630 V.

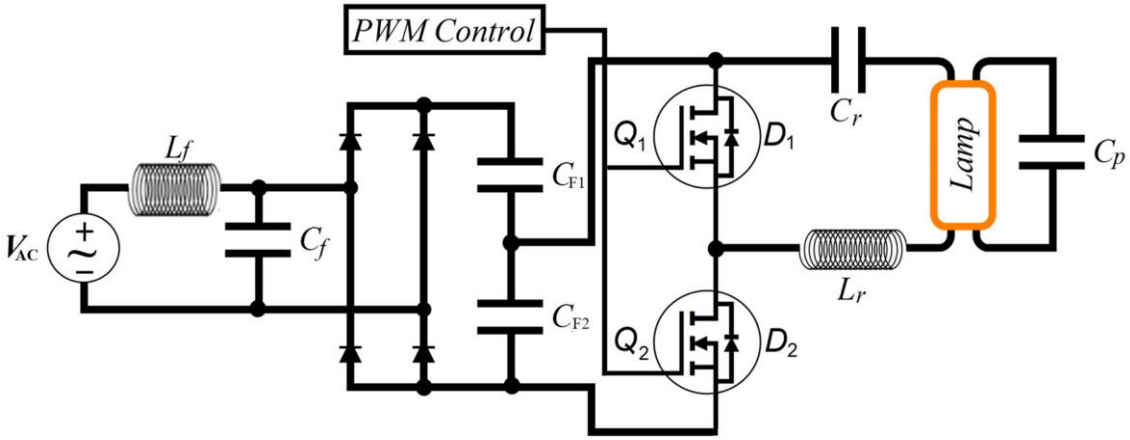

Figure 4. Electronic ballast structure using a conventional converter

Figure 5 depicts the voltage and the arc current of the discharge lamp. The voltage and the arc current of the discharge lamp are modulated at a frequency of 50 kHz and are contained in an envelope which oscillates at 1 kHz with a modulation rate (maximum value / value minimum) equal to approximately 5 and that the effective value of the arcing current of the lamp oscillates at the frequency of the envelope of the supply current which is evaluated at 1kHz. The THDs of the arc voltage and arc current of our discharge lamp are equal to 6.51% and 10.41%, respectively (as shown in Figure 6). A direct consequence of this ripple in the rms current value is a decrease in the mean time between system failures, as well as deterioration in lamp efficiency and effectiveness in germicidal treatment.

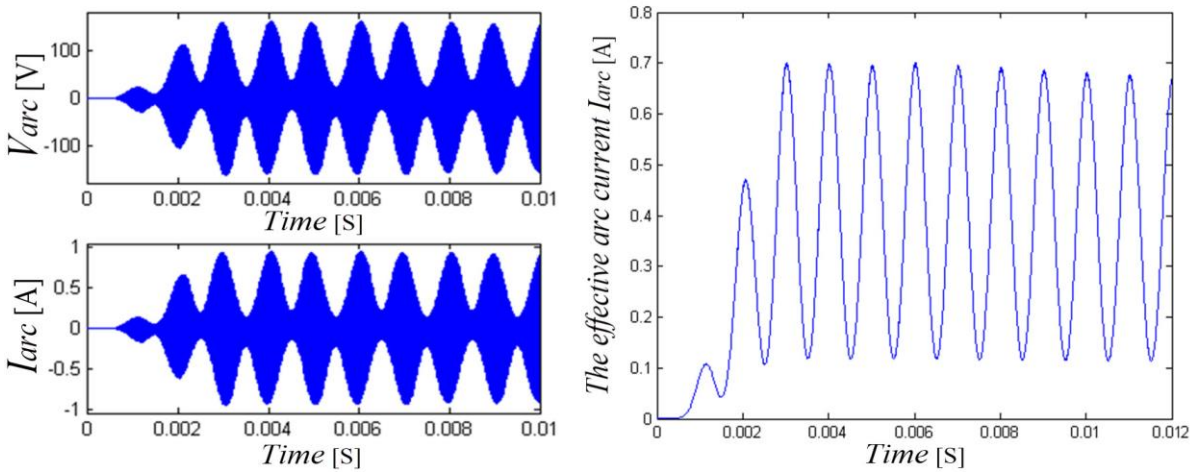

Figure 5. Representation of currents and arc voltage of the discharge lamp

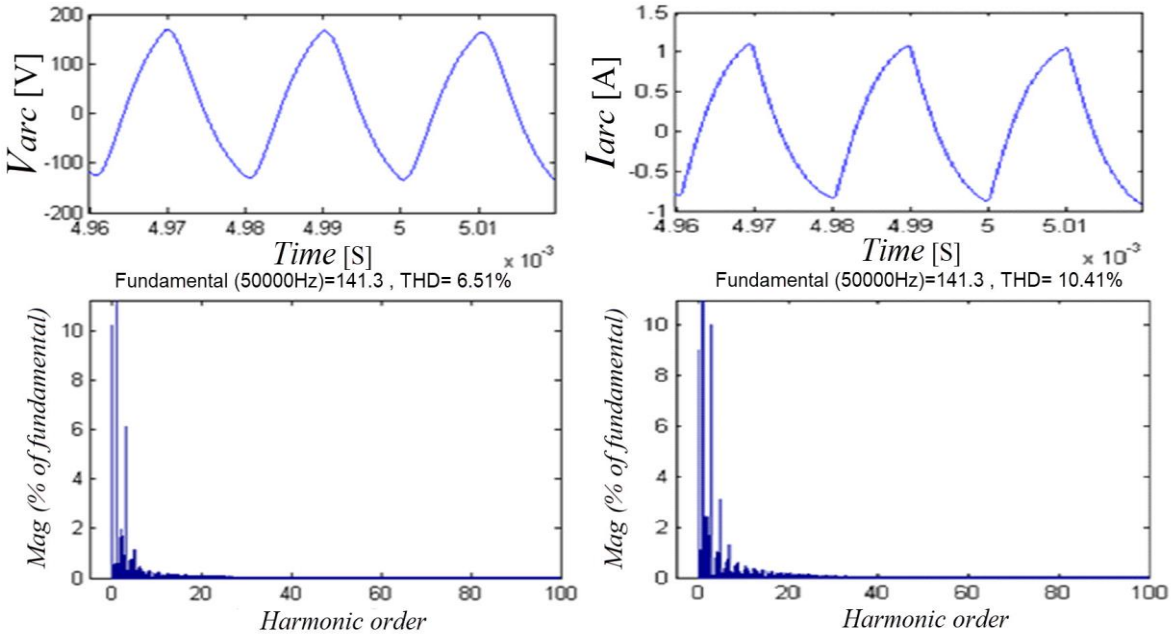

Figure 6. Distortion rate of discharge lamp arc voltage and current

These poor performances of the open-loop system lead us to consider a closed-loop system with PI regulator of the arc current (Aissa- Bokhtache et al., 2016). The block diagram of the system with PI controller is illustrated in Figure 7.

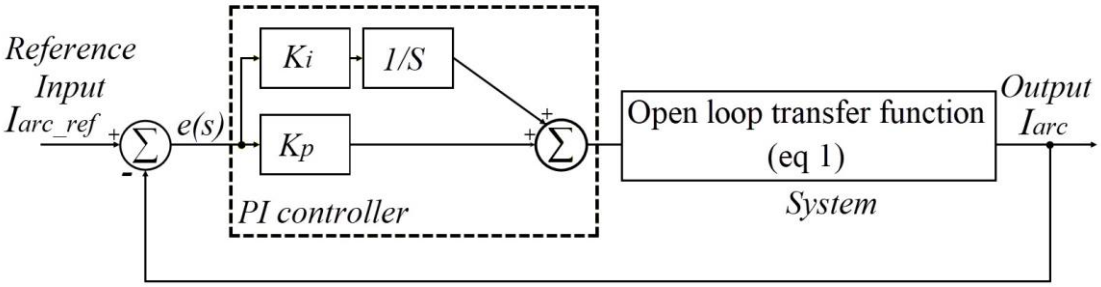

Figure 7. Closed-loop control system with PI controller

The transfer function C(S) of the proportional-integral controller is given by:

$$C(S) = K_p + \frac{K_i}{S} \tag{2}$$

Where: K_p, and K_i are the controller gains calculated using pole placement method, K_p = 0.0081 and K_i = 0.0091. The closed-loop transfer function (TFCL) of the system can be calculated by:

$$TFCL(S) = \frac{C(S).G(S)}{1 + C(S).G(S)} \tag{3}$$

Where: $G(s)$ is the open-loop transfer function of the system.

Figure 8 depicts the voltage and the arc current of the discharge lamp in closed-loop control system with PI controller. The figure clearly shows the improvements made to the waveforms compared with those of the open-loop simulation (Figure 5). Indeed the introduction of the PI in the closed loop eliminated the oscillations of the envelopes, one notes that after the transitory mode, the amplitudes become constant and the system is more stable.

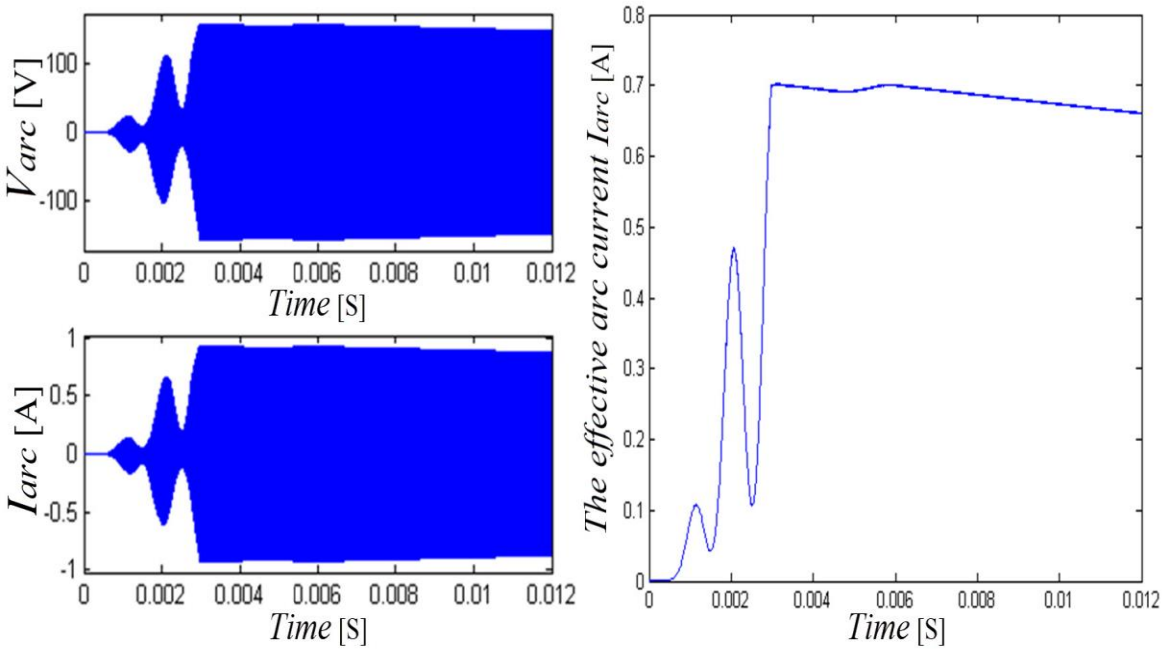

Figure 8. Closed-loop control system with PI controller

Power Supply of the System by a Multicell Converter

Figure 9 depicts the system with a multicell converter. It is an inverter assembly with multiple cells of a switching type cell (with a capacitive midpoint). This structure is composed of (P = 4) switching cells, separated from each other by P-1= 3 floating capacitors. The five voltage levels obtained by this inverter give it frequency advantages and allow it to obtain a good current source, of high quality both in terms of waveform and frequency response (Aissa-Bokhtache et al., 2020; Aissa-Bokhtache et al., 2021; Aimé et al., 2004). Characteristics of the Midpoint Series Four Cell Inverter (Aissa-Bokhtache et al.,2023) are:
E = 800 V, $C_1 = C_2 = C_3 = 5$ nF, $f_{dec} = 3{,}2$ MHz, $f_{mod} = 50$ KHz.

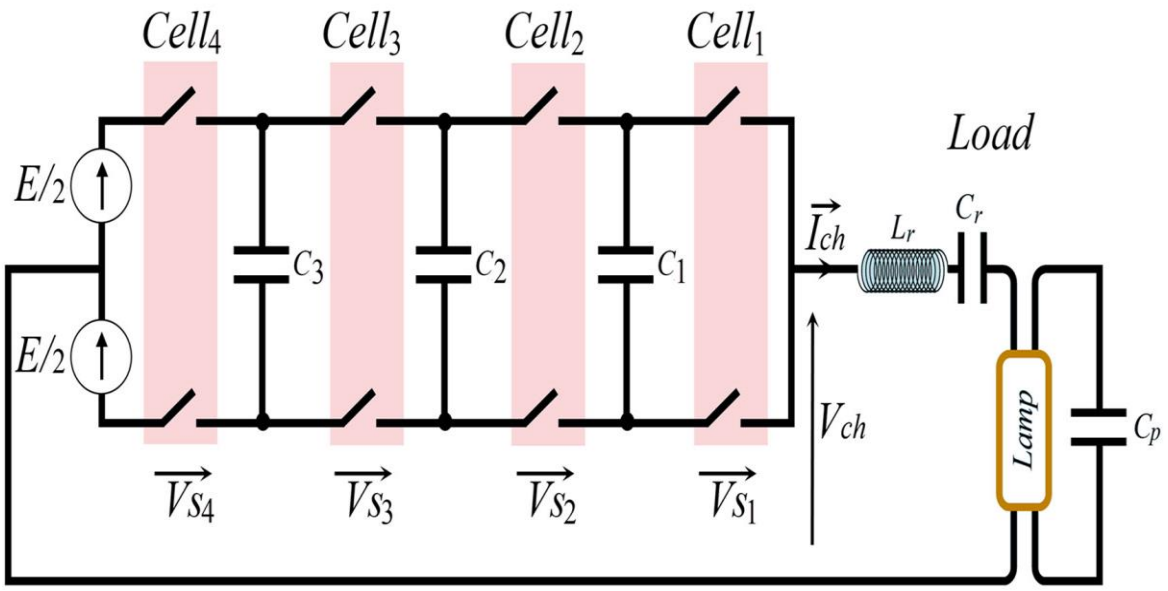

Figure 9. Voltage Source Midpoint Series Four Cell Inverter

The instantaneous modeling of the converter gives us the following system of equations:

$$\begin{cases} \dfrac{dV_{C_1}}{dt} = \dfrac{1}{C_1}\left(u_2 - u_1\right) I_{LOAD} \\ \dfrac{dV_{C_2}}{dt} = \dfrac{1}{C_2}\left(u_3 - u_2\right) I_{LOAD} \\ \dfrac{dV_{C_3}}{dt} = \dfrac{1}{C_3}\left(u_4 - u_3\right) I_{LOAD} \\ V_{LOAD} = \left(\left(u_1 - u_2\right) V_{C_1} + \left(u_2 - u_3\right) V_{C_2} + \left(u_3 - u_4\right) V_{C_3} + u_4\, E - \dfrac{E}{2} \right) \end{cases} \tag{4}$$

We use the direct command to control the switches. Direct control aims to maintain the voltages across the floating capacitors at their desired reference values, both in static and dynamic conditions. Also, it ensures that the output voltage of the converter meets the required discrete level. To achieve this, the control algorithm considers two key factors:

1- Knowledge of the required discrete voltage level: The control algorithm takes into account the specific voltage level needed at the converter's output. The output voltage can have (p + 1) possible values, with each level ideally having a predetermined amplitude.

$$V_j = j \times \frac{E}{p}, \qquad j = 0,1,2,.....p \tag{5}$$

2- Knowledge of the state of the floating capacitors' voltages relative to their equilibrium values: The control algorithm also considers the voltages across the floating capacitors and their relationship to the desired equilibrium state. Each floating capacitor can be in one of three states:

- ✓ Equilibrium state: Capacitor's voltage level falls within an allowable range around its equilibrium value.
- ✓ State of higher imbalance: The capacitor's voltage level exceeds the allowable range.
- ✓ State of lower imbalance: The capacitor's voltage level falls below the allowable range.

Table 2 gives the theoretical output voltage V_{ch}, charging or discharging capacitors (C_1, C_2, C_3) according to the control of the switches (u_1, u_2, u_3, u_4) and the direction of the current (+*I*, -*I*).

Table 2. Output voltage level with corresponding conducting switches

Output voltage V_{ch}					Switch control				Balancing capacitors						Nº
-E/2	-E/4	0	E/4	E/2	U_1	U_2	U_3	U_4	C_1 +*I*	C_1 -*I*	C_2 +*I*	C_2 -*I*	C_3 +*I*	C_3 -*I*	
×					0	0	0	0	0	0	0	0	0	0	1
	×				0	0	0	1	0	0	0	0	+	-	2
	×				0	0	1	0	0	0	+	-	-	+	3
		×			0	0	1	1	0	0	+	-	0	0	4
	×				0	1	0	0	+	-	-	+	0	0	5
		×			0	1	0	1	+	-	-	+	+	-	6
		×			0	1	1	0	+	-	0	0	-	+	7
			×		0	1	1	1	+	-	0	0	0	0	8
	×				1	0	0	0	-	+	0	0	0	0	9
		×			1	0	0	1	-	+	0	0	+	-	10
		×			1	0	1	0	-	+	+	-	-	+	11
			×		1	0	1	1	-	+	+	-	0	0	12
		×			1	1	0	0	0	0	-	+	0	0	13
			×		1	1	0	1	0	0	-	+	+	-	14
			×		1	1	1	0	0	0	0	0	-	+	15
				×	1	1	1	1	0	0	0	0	0	0	16

Table 2 illustrates that the converter is capable of generating five distinct voltage levels. However, to achieve better accuracy in controlling discharge lamps, it is advantageous to generate seventeen voltage values. This can be accomplished by employing four voltage levels during a single switching period, allowing for more precise control. Figure 10 depicts the schematic representation of the voltages to be generated; the top portion shows the voltages that can be generated using the five basic levels, while the bottom portion displays the voltage thresholds necessary for controlling the switches.

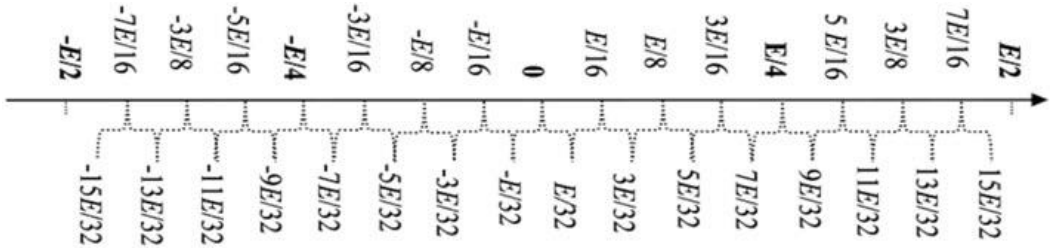

Figure 10. Schematic representation of the voltages to be generated

In the following figures we present the simulation results concerning a series multicell inverter formed by four midpoint cells, supplying the discharge lamp. Figure 11 depicts the curves of discharge lamp Arc voltage and current. RMS Arc current and flying capacitors voltages are shown in Figure 12.

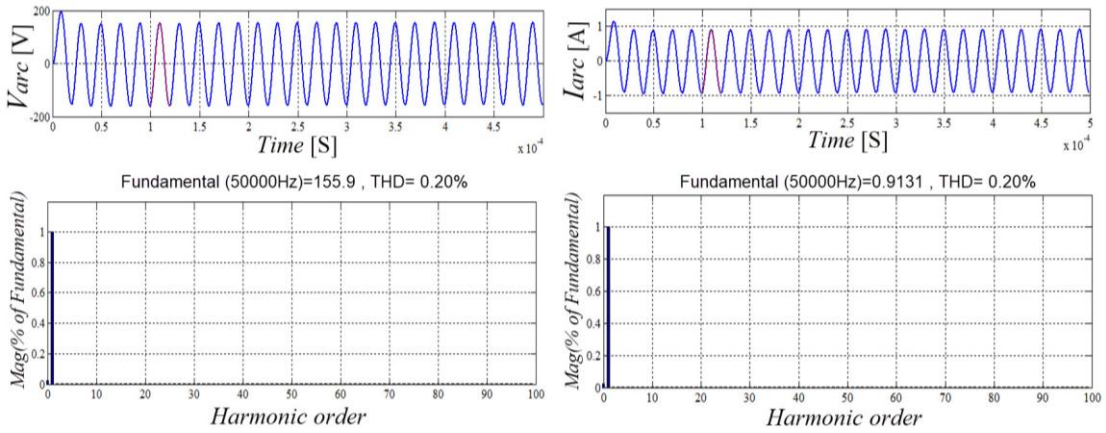

Figure 11. Discharge lamp arc voltage and current

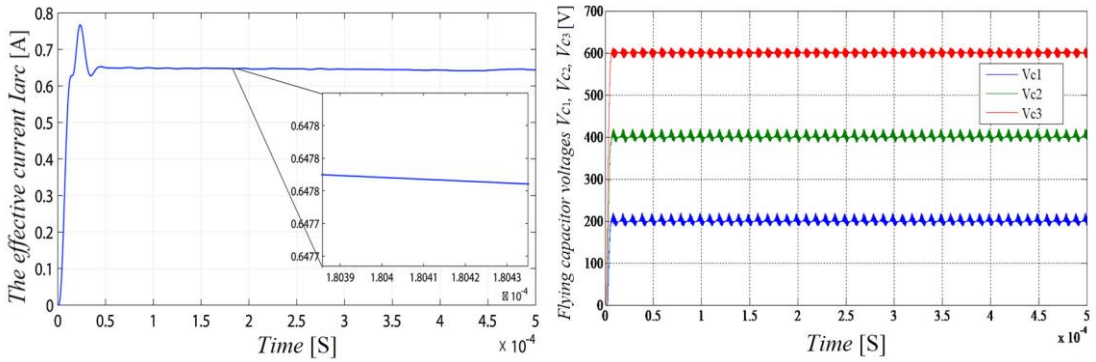

Figure 12. (a) RMS arc current, (b) Flying capacitor voltages

According to Figure 11, the waveforms of the arc voltage and current are sinusoidal, their frequencies are identical to the frequency of the modulating (50kHz) with a harmonic distortion rate of 0.20% for both. This means that the arc voltage and arc current are in phase. This means that the discharge lamp behaves like a simple resistor in arc mode. We also note in Figure 12(a) that the effective value of the arc current has actually reached the desired value which is 0.65A after 40 µs with an accuracy of 0.001A. According to the Figure 12(b), voltages at the terminals of the floating capacitors stabilizes at the values (k×E/P) corresponding to Vc_1 = 200V, Vc_2 = 400 V, and Vc_3 = 600 V, at the instant (20 µs). the effective arcing current stabilizes at 0.65 A (desired value) after 60 µs.

The introduction of a classic PI in the closed loop of the system has significantly improved the THDs, as shown in the following Figures. Figure13 depicts the lamp Arc voltage and current and their Harmonic spectrum with PI regulator. Figure 14 depicts the RMS arc current of the lamp with a PI regulator.

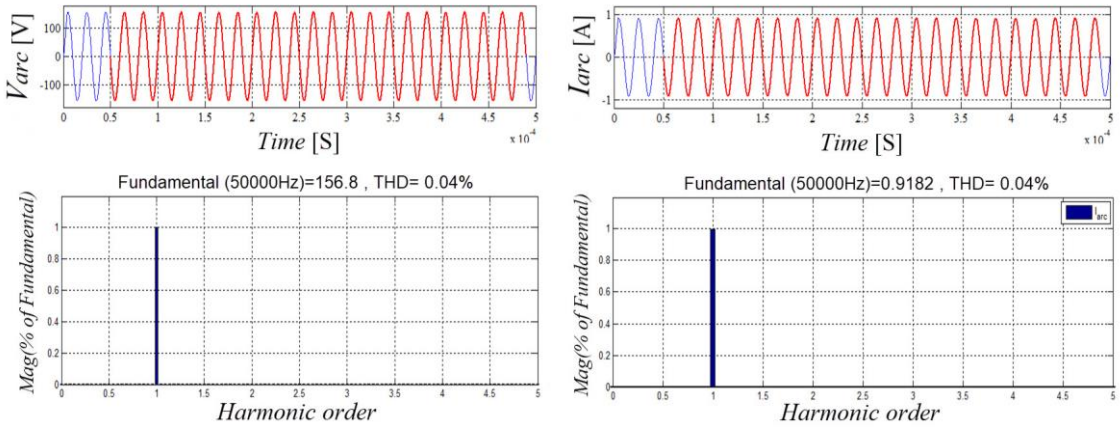

Figure 13. Lamp Arc voltage and current and their Harmonic spectrum with PI regulator

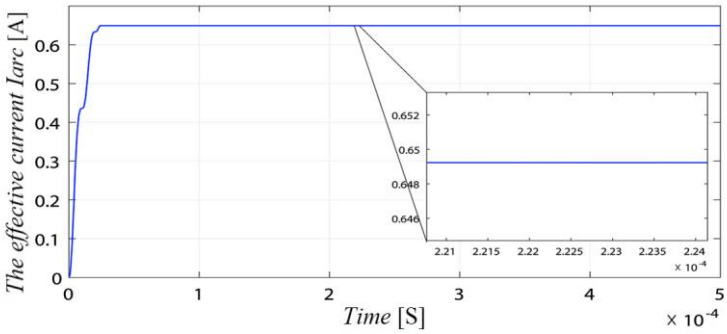

Figure 14. RMS arc current of the lamp with a PI regulator

We note that the arc current perfectly follows the sinusoidal reference that we imposed on our lamp (the frequency = 50 KHz), in Figure 13, with response time of 27 µs to reach 0.65 A depicted in effective value curve in Figure 14. We also notice a considerable improvement on the THD level which is 0.04% compared to the simulation on open loop which is 0.20%.

Power Supply of the System by a Matrix Converter

Figure 15 depicts the system with a Matrix converter. This converter is characterized by a matrix topology of four switches (matrix [2x2]), (Toumi et al., 2013), such that the two input phases of the network are interconnected to the two output phases of the converter by means of bidirectional power switches (Zuckerberger et al., 1997; Friedli et al., 2012).

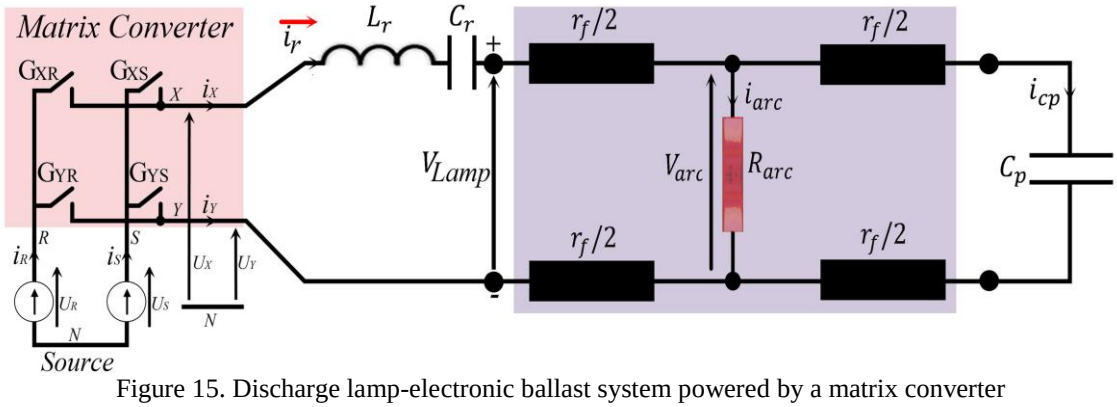

Figure 15. Discharge lamp-electronic ballast system powered by a matrix converter

Figure16 shows the lamp arc current and voltage waveforms and their THDs. Note that the arc voltage and current envelopes oscillate at a frequency of 100 Hz. Curves show that the arc current and voltage oscillate at the desired frequency which is 50 kHz with a distortion rate of 1.98% for the arc current and the arc voltage. Also, we note that the current and the voltage are totally in phase with the same THD. This is explained by the fact that the electric arc of the lamp is characterized by a resistance R_{arc}. The voltage and current waveforms are perfectly sinusoidal in steady state operation.

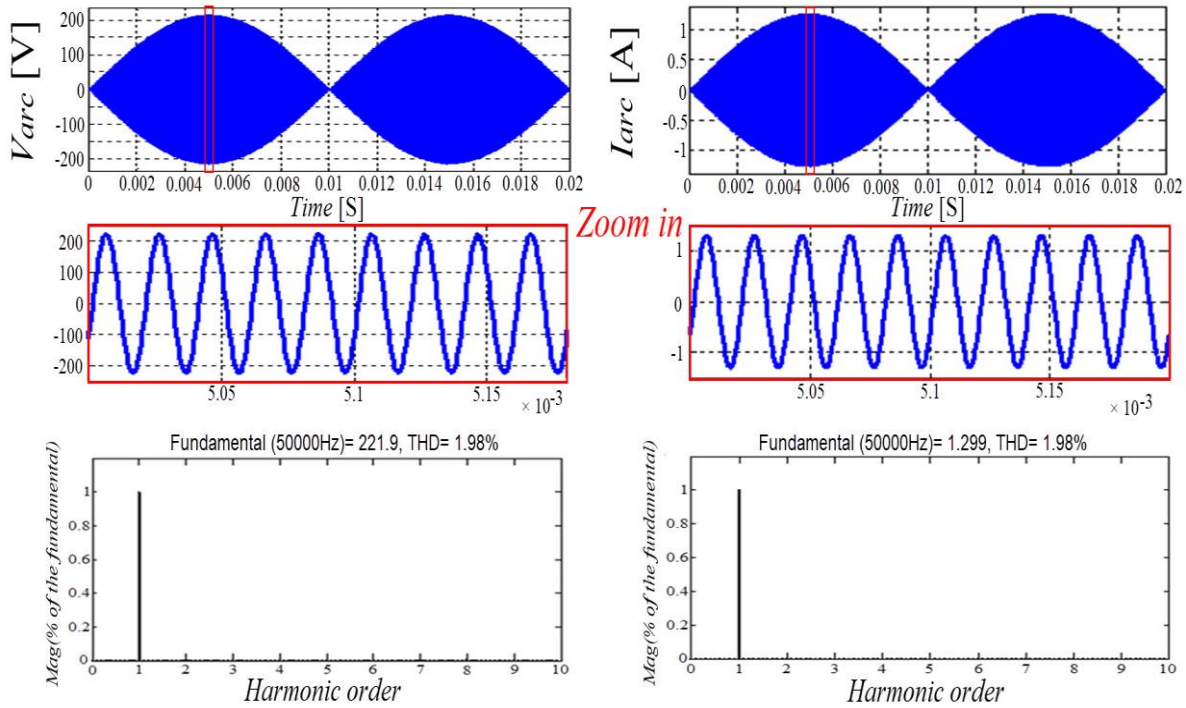

Figure 16. Waveforms of arc current and voltage of the lamp and their harmonic spectrum in open-loop

Figure 17 depicts the RMS arc current in open-loop case, when the system is powered by a matrix converter. The curve shows that the effective arc current is stabilized at 0.65A (the desired value) after a transient state of about 0.0195 Seconds.

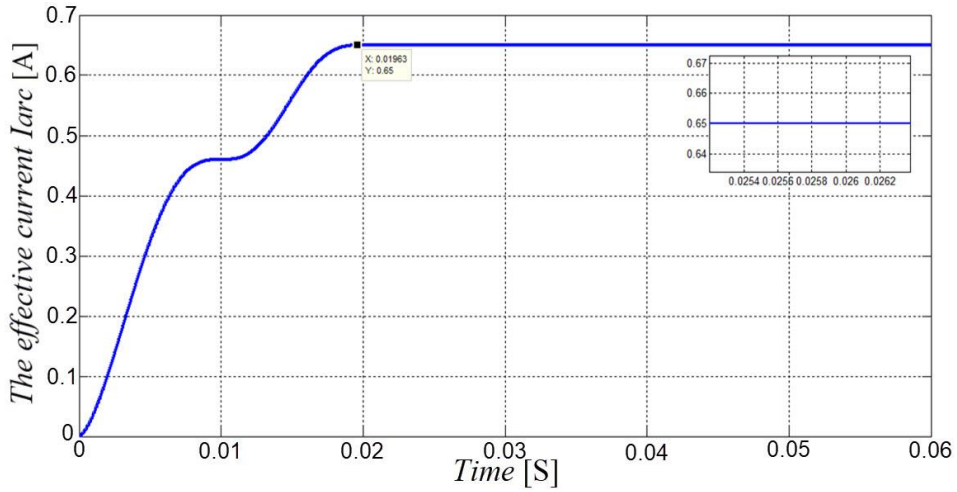

Figure 17. RMS arc current in open-loop

As the previous two cases using the conventional and the multicell converters, we impose arc current regulation using matrix converter with a reference of 0.65A. The difference will be transformed into the switching frequency of the switches. We use the pole placement method to calculate the gains of the classical PI controller. The calculated K_P and K_I values are: $K_P = 5.345\times10^{20}$ and $K_I = 3.095\times10^{24}$. Figure 18 illustrates the waveforms of arc current and voltage of the lamp and their harmonic spectrum in closed-loop case.

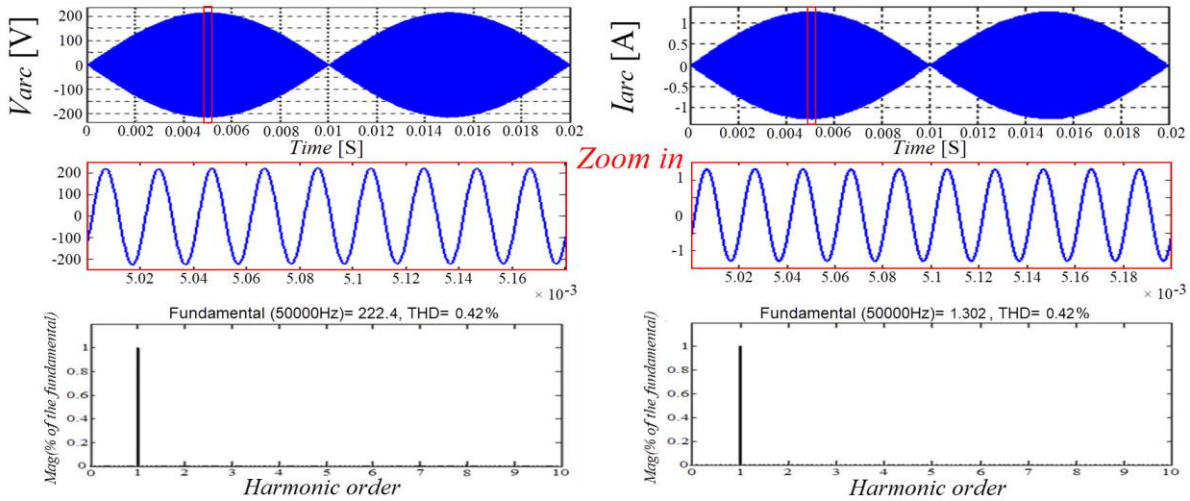

Figure 18. Waveforms of arc current and voltage of the lamp and their harmonic spectrum in closed-loop

We can see from the Figure 18 that the arc current and the arc voltage are totally in phase with the same THD. The voltage and current waveforms are perfectly sinusoidal in steady state with a frequency of 50 kHz. The THD is improved (0.42% with introduction of the PI in the regulation loop against 1.98% in open-loop). Figure 19 shows the RMS arc current in closed-loop case, when the system is powered by a matrix converter. The effective arc current is stabilized at 0.65A (the desired value) after a transient state of about 0.01 Seconds.

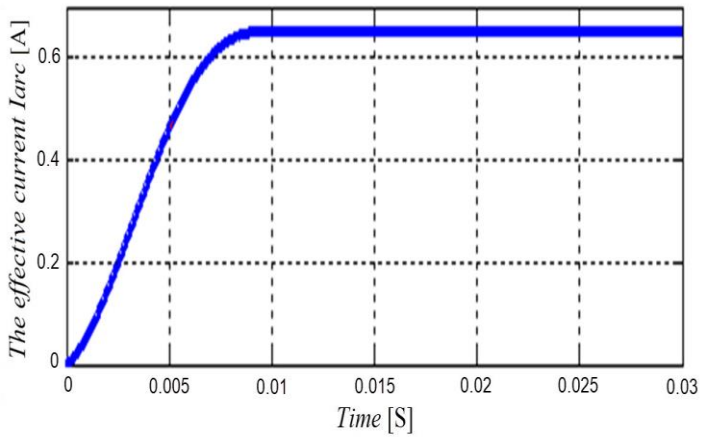

Figure 19. RMS arc current in closed-loop

Results Comparison

To clearly illustrate the advantages of the converter topologies discussed, a comparative analysis has been conducted between the conventional converter, multi-cell converter, and matrix converter, as summarized in Table 3. The key parameters evaluated for comparison include transient response (in milliseconds) and total harmonic distortion (THD). From Table 3, we observe that the results obtained using the series multicellular converter are the best, as it behaves like a good current source, delivering a sinusoidal current at its output (with almost zero THD), without ripples even in open-loop.

Table 3. Comparison between the results of the three converters

Type of converter		Waveforms	THDs (%)	Transient regime (ms)
Classic Converter	Open-loop	*arc* current ripple with 1 kHz	10.41	2.5
	Closed-loop	Eliminates of *Iarc RMS* oscillations	5.59	3
Multi-cell Converter	Open-loop	Sinusoidal signal without envelope	0.20	0.043
	Closed-loop	Waveform improvement	0.04	0.025
Matrix Converter	Open-loop	Envelope of 100 Hz	1.98	19.5
	Closed-loop	Envelope of 100 Hz	0.42	9.5

Conclusion

The objective of this study was to develop the most optimal current source for powering the discharge lamp-electronic ballast system used in water purification. The serial multicell converter functions as an efficient current source, delivering a sinusoidal current with nearly zero THD and no ripple, even in open-loop operation. It operates at a frequency of 50 kHz with an RMS value of 0.65 A, generating maximum UV radiation at 253.7 nm. This ensures optimal power delivery to the system, resulting in an effective germicidal action.

Scientific Ethics Declaration

The authors declare that the scientific ethical and legal responsibility of this article published in EPSTEM Journal belongs to the authors.

Acknowledgements or Notes

* This article was presented as an poster presentation at the International Conference on Technology, Engineering and Science (www.icontes.net) held in Antalya/Turkey on November 14-17, 2024.

References

Aimé, M., Gateau, G., & Fadel, M. (2004). Commande des convertisseurs multi cellulaires série à fréquence fixe en mode courant : Control of serial multi-cellular converters at fixed frequency in current mode. *CIFA'04, Douz, (Tunisie)*, 22–24.

Aissa-Bokhtache, A., Zegaoui, A., Kellal, M., Boucherit, M.S., Belmadani, B., & Aillerie, M. (2016). Optimization based on fuzzy logic control of discharge lamp-electronic ballast system for water purification. *Electric Power Components and Systems*, *44*, 1981–1990.

Aissa-Bokhtache, A., Zegaoui, A., Belmadani, B., & Boucherit, M.S. (2015). Water purification by a lamp discharge-electronic ballast system using a full bridge inverter. *Energy Procedia*, *74*, 446–452.

Aissa-Bokhtache, A., Zegaoui, A., Aillerie, M., Djahbar, A., Allouache, H., Hemici, K., Kessassia, F.Z, & Bouchrit, M. S. (2017). Power supply improvements for ballasts-low pressure mercury/argon discharge lamp for water purification. *AIP Conference Proceedings 1814*, 020059, doi: 10.1063/1.4976278.

Aissa-Bokhtache, A., Zegaouia, A., Taleb, R., & Aillerie, M. (2021). Control of an electronic ballast-discharge lamp system supplied by a multicellular converter dedicated to water purification. *Desalination and Water Treatment, 228*, 176–186.

Aissa - Bokhtache, A., Zegaoui, A., Taleb, R., & Aillerie, M. (2020). Super twisting sliding mode control algorithm of a discharge lamp for water sterilization. *Kansai University Reports*, *62*(4), 1731- 1741.

Aissa - Bokhtachte, A., Latroch, M., Toualbia, A., Djafer, L., & Benallou, M. (2023). Modern control of a power supply based on a matrix converter for water disinfection by UVC radiation. *The Eurasia Proceedings of Science, Technology Engineering & Mathematics (EPSTEM), 26*, 733-740.

Aissa- Bokhtache, A., Latroch, M., Toualbia, A., Toubal Maamar, A. E., & Boucherit, M. S. (2023). Optimization of a power supply using 3 types of converters of a discharge lamp-electronic ballast system for water purification. *Proceedings of 2nd International Conference on Electronics, Energy and Measurement (IC2EM)*, 1-6.

Amet, L., Ghanes, M., & Barbot, J.P. (2011). Direct control based on sliding mode techniques for multicell serial chopper. *Proceedings of the 2011 American Control Conference (ACC)*, 751–756.

Costache, M. C., Damelincourt, J.J., & Zissis, G. (2000). Optimisation of an ultraviolet source working in a consumer water reactor. *UVX 2000 Colloque Sur Les Sources Cohérentes et incohérentes UV, VUV, et X – Applications et Développements Récents*, *87*(5), 65–66.

De Oro, L. A., Melo, G. de A., & Canesin, C. A. (2014). UV dose investigation for imersed lamp purifier for electronic ballast UV lamps design. *IEEE 16th International Power Electronics and Motion Control Conference and Exposition (PEMC)*, 893-900.

Friedli, T., & Kolar, J. W. (2012). Milestones in matrix converter research. *IEEJ Journal of Industry Applications*, *1*(1), 2-14.

Holmes, D. G., & Lipo, T. A., (1992). Implementation of a controlled rectifier using ac-ac matrix converter theory. *IEEE Transactions on Power Electronics*, *7*(1), 240-250.

Toumi, A., Chhun, L., Bhosle, S., Zissis, G., Maussion, P., & Hirsch, J. (2013). Acoustic resonance characterization and numerical model including acoustic streaming in an HPS lamp. *IEEE Industry Applications Society Annual Meeting, 49*, 1154–1160.

Zuckerberger, A., Weinstock, D., & Alexandrovitz, A. (1997). Single-phase matrix converter. *IEE Proceedings - Electric Power Applications, 144*(4), 235-240.

Author Information

Aicha Aissa -Bokhtache
Laboratoire Génie Electrique et Energies Renouvelables (LGEER), Electrical Engineering Department, Hassiba Benbouali University of Chlef
BP. 151, Hai Essalam, 02000 Chlef, Algeria
Contact e-mail: *ahcial71@gmail.com*
a.aissabokhtache@univ-chlef.dz

Maamar Latroch
Laboratoire Génie Electrique et Energies Renouvelables (LGEER), Electrical Engineering Department, Hassiba Benbouali University of Chlef
BP. 151, Hai Essalam, 02000 Chlef, Algeria

Nadia Badni
Center of Scientific and Technical Research in Physico-chemical Analysis of Tipaza (CRAPC),
BP. 384, Ex-Pasna Industrial Zone, Bou-Ismail PO Box 42004, Tipaza, Algeria.

Alla Eddine Toubal-Maamar
Department of Electrical Systems Engineering, Faculty of Technology, University of M'hamed Bougara of Boumerdes Frantz Fanon city, 35000 Boumerdes, Algeria

Lemya Djafer
Laboratoire Génie Electrique et Energies Renouvelables (LGEER), Electrical Engineering Department, Hassiba Benbouali University of Chlef
BP. 151, Hai Essalam, 02000 Chlef, Algeria

Amina Merini
Laboratoire Génie Electrique et Energies Renouvelables (LGEER), Electrical Engineering Department, Hassiba Benbouali University of Chlef
BP. 151, Hai Essalam, 02000 Chlef, Algeria

To cite this article:

Aissa-Bokhtache, A., Latroch, M., Badni, N., Toubal-Maamar, A.E., Djafer, L., & Merini, A. (2024). Comparative analysis of three converters providing power to a discharge lamp-electronic ballast system designed for water sterilization. *The Eurasia Proceedings of Science, Technology, Engineering & Mathematics (EPSTEM), 32*, 53-65.